SUPPORTING INFORMATION

Hydrodynamic Solvent Coupling Effects in Quartz Crystal Microbalance Measurements of Nanoparticle Deposition Kinetics

Zbigniew Adamczyk*, Marta Sadowska

Jerzy Haber Institute of Catalysis and Surface Chemistry, Polish Academy of Sciences, Niezapominajek 8, 30 - 239 Krakow, Poland.

Corresponding author, e-mail: ncadamcz@cyf-kr.edu.pl

E-mail addresses: ncadamcz@cyf-kr.edu.pl (Z. Adamczyk), ncsadows@cyf-kr.edu.pl (M. Sadowska)

Table of contents:

1. **Basic characteristic of the polymer particles.**

Table S1. Basic physicochemical parameters of the polymer particles used in this work: pH 4.0, $I = 10^{-2}$ M, NaCl, $T = 298$ K.

Particle suspension	d_p [nm] DLS	d_p [nm] AFM	d_p [nm] diffr.	ζ [mV] LDV
A20	26±2	25±4	-	71±2
L40	39±3	39±3	-	-82±3
A70	67±5	73±7	73±7	74±2
A140	140±10	140±12	140±12	79±3

Footnotes: particle density ρ_p = 1.05 g cm^{-3}, d_p - particle diameter (DLS - dynamic light scattering, AFM - atomic force microscopy, diffr. - laser diffractometry), ζ - zeta potential derived from LDV (electrophoresis).
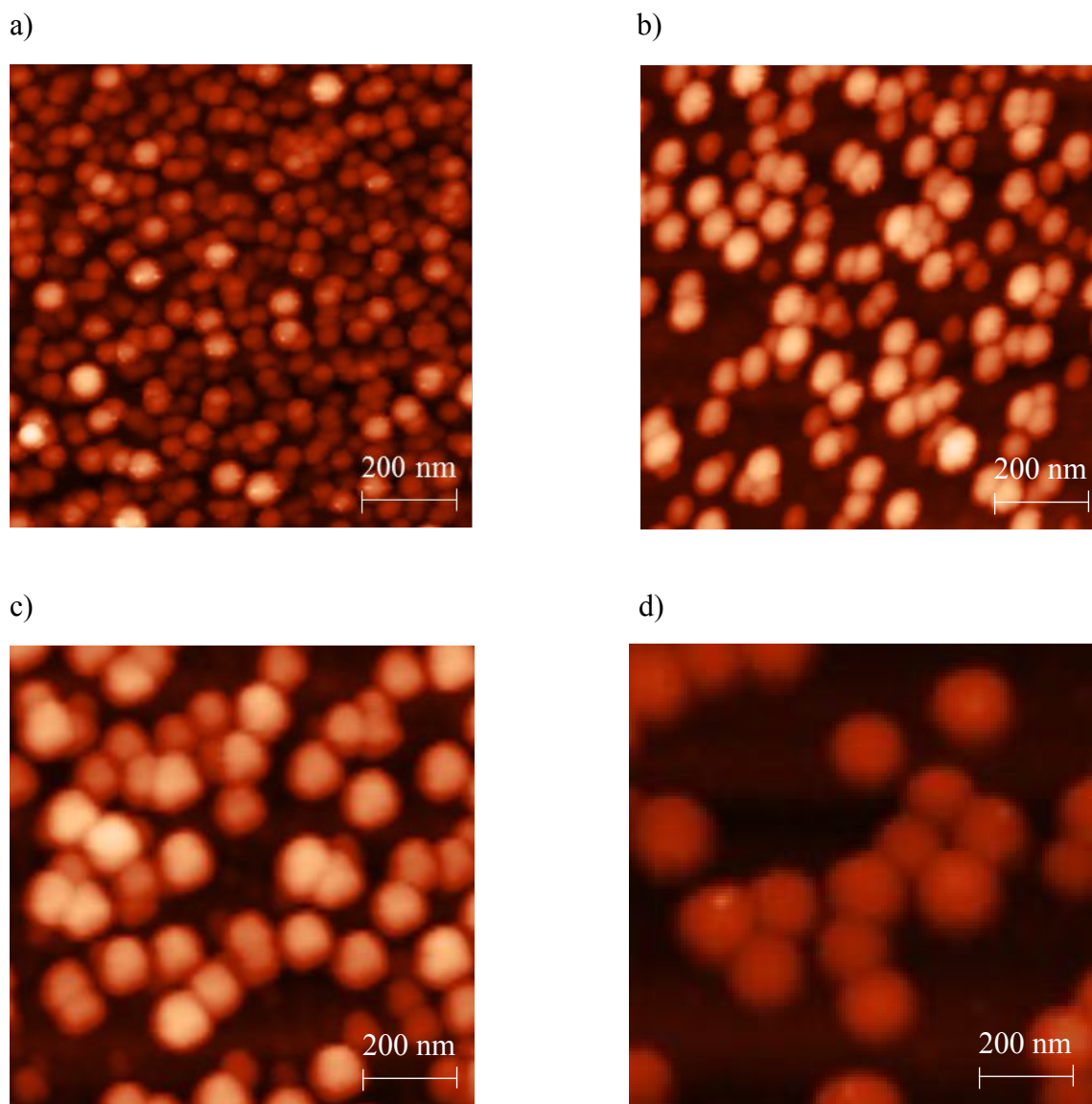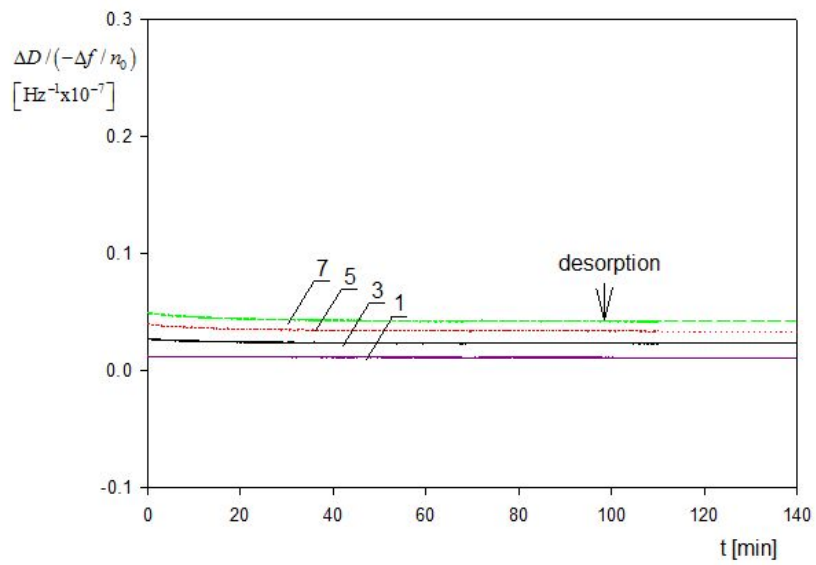
a)

b)

200 nm

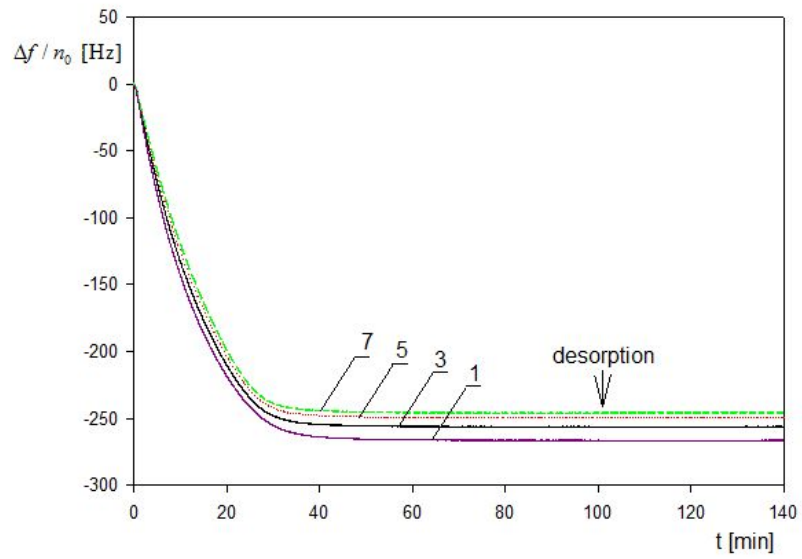200 nm

c)

d)

200 nm

200 nm

Figure S1. Monolayers of different particles used in this work adsorbed on the silica sensor, acquired by AFM, part a) the A20 particles, surface coverage 0.15, b) the L40 particles surface coverage 0.18 c) the A70 particles, surface coverage 0.25 d) the A140 particles surface coverage 0.25

2. The primary QCM adsorption runs.

a)

b)
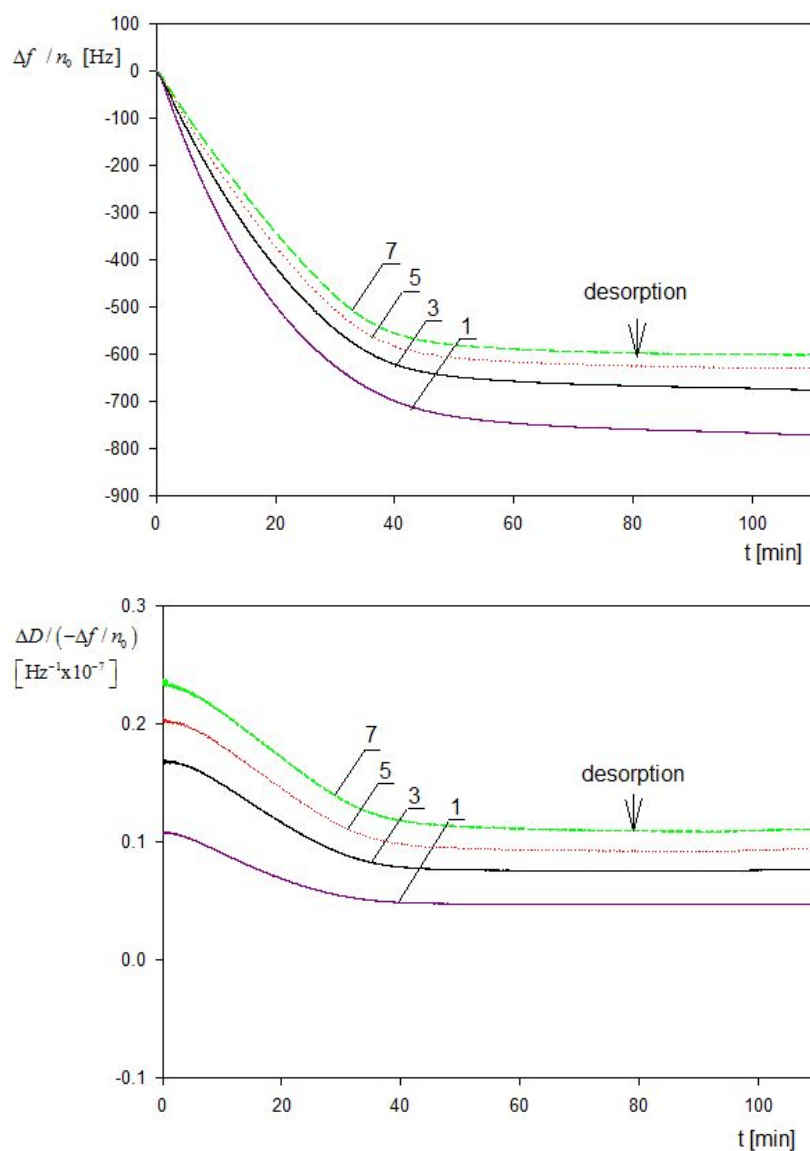
Figure S2. The primary adsorption runs for polymer particles derived from QCM-D measurements and expressed in terms of the frequency change $\Delta f/n_o$ and the ratio of dissipation to frequency change $\Delta D/(-\Delta f/n_o)$ for various overtones 1,3,5,7; silica sensor, ionic strength 0.01 M, pH 4, volumetric flow rate 2.5x10^{-3} cm^3 s^{-1}, Part a) the A70 suspension, bulk concentration 20 mg L^{-1}. Part b) the A140 suspension, bulk concentration 100 mg L^{-1}.

3. **The hydrodynamic boundary layer over an oscillating plate**

The fluid velocity distribution over a plate undergoing harmonic oscillations in the tangential direction characterized by the angular velocity $\omega = 2\pi f$ (where f is the oscillation frequency) in a Newtonian liquid is given by[1]

$$V_x = V_0\, e^{-\left(\frac{\omega}{2v}\right)^{1/2} z} \sin\left(\omega\, t - \left(\frac{\omega}{2v}\right)^{1/2} z\right) \tag{S1}$$

where V_0 is the amplitude of plate velocity oscillations, v is the kinematic viscosity of the fluid, z is the vertical distance from the plate.

Eq.(S1) indicates that the fluid velocity exponentially decreases with the distance z proportionally to the square root of the angular velocity.

Let us calculate the distance where the flow amplitude decreases (compared to the plate velocity) by the factor denoted by f_v. Using Eq.(S1) this factor can be expressed as

$$\delta = \left(\frac{2v}{\omega}\right)^{1/2} \ln(f_v^{-1}) \tag{S2}$$

for $\ln(f_v^{-1}) = 1$ one has $\delta = \delta_h = \left(\frac{2v}{\omega}\right)^{1/2}$, which is commonly considered as a hydrodynamic boundary layer thickness[1].

In Table S2 the distances and the hydrodynamic boundary layer thickness for the fundamental frequency of 5×10^6 s^{-1} (Hz) pertinent to our QCM-D measurements are collected for various overtones. One can notice that the flow amplitude decreases to 0.5 of the maximum plate amplitude at the distance equal to 165 nm for the fundamental frequency. For the 7th overtone this distance is equal to 62.4 nm. Analogously, one can notice that the amplitude decreases to only 0.1 of the plate amplitude at the distance of 548 and 207 nm for the fundamental frequency and the 7th overtone, respectively. Thus, at distances larger than those mentioned there appears a stagnant core region, where the flow vanishes.

Table S2. Hydrodynamic boundary layer thickness for oscillating solid plates (sensors) in aqueous media for the fundamental frequency 5×10^6 s^{-1} (Hz).

overtone number, n_0	$\omega = 2\pi f\, n_0$ [s^{-1}]	$\delta_{0.5}$ [nm]	δ_h [nm]	$\delta_{0.1}$ [nm]
1	3.14×10^7	165	238	548
3	9.42×10^7	95.3	137	316
5	1.57×10^8	73.8	106	245
7	2.2×10^8	62.4	90.0	207
11	3.45×10^8	49.7	71.6	165

Footnotes: temperature 298 K, kinematic viscosity 0.00893 cm^2 s^{-1}

$\delta_{0.5}$ - the distance where the amplitude decreases to 0.5 of the plate amplitude

δ_h - the hydrodynamic boundary layer thickness
        (the amplitude decreases to $1/e = 0.3679$)

$\delta_{0.1}$ - the distance where the amplitude decreases to 0.1 of the plate amplitude

A graphical comparison of the comparison of the polymer particle sizes used in this work with the hydrodynamic boundary layer thickness for the 1st and the 7th overtone is presented in Figure S4.
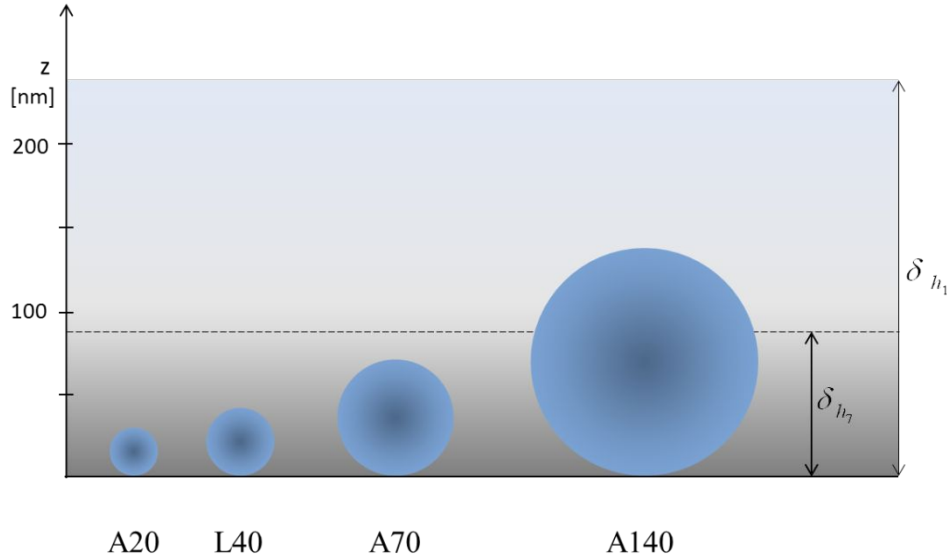

Figure S3. The polymer particle size compared with the hydrodynamic boundary layer thickness calculated for the 1-st and the 7th overtones, and equal to 238 and 90 nm, respectively.

From Eq.(S1) one can deduce that the flow shear rate is given by[1]

$$G_{Sh} = \frac{\partial V_x}{\partial z} = \left(\frac{\omega}{v}\right)^{1/2} V_0\, e^{-\left(\frac{\omega}{2v}\right)^{1/2} z} \sin\left[\omega t - \left(\frac{\omega}{2v}\right)^{1/2} z + \frac{\pi}{4}\right] \tag{S3}$$

Consequently, the shear rate amplitude attains the maximum value of $\left(\frac{\omega}{v}\right)^{1/2} V_0$ at the plate surface and exponentially decreases with the distance from the surface with the characteristic decay rate equal to the hydrodynamic boundary layer thickness. At the distance equal to particle radius a_p the shear rate amplitude normalized by the surface amplitude $\overline{G}_{Sha}$ is given by

$$\overline{G}_{Sha} = e^{-\left(\frac{\omega a_p^2}{2v}\right)^{1/2}} = e^{-a_p/\delta_h} = f_{Sh} \tag{S4}$$

where f_{Sh} is the dimensionless correction factor, which only depends on the ratio of the particle to the hydrodynamic boundary layer thickness. This correction factor calculated for various particle sizes as a function of the overtone number are collected in Table S3.

Table S3. The correction factor to the shear rate f_{Sh} calculated for various particle sizes as a function of the overtone number in aqueous media, for the fundamental frequency equal to 5×10^6 s^{-1} (Hz).

Particle \ Overtone Number n_0	A20 d_p= 26 nm	L40 d_p= 39 nm	A70 d_p= 73 nm	A140 d_p= 140 nm
1	0.95	0.92	0.86	0.75
3	0.91	0.87	0.77	0.60
5	0.88	0.83	0.71	0.52
7	0.86	0.80	0.67	0.46
9	0.85	0.78	0.63	0.41
11	0.83	0.76	0.60	0.38

Footnotes: the temperature 298 K, the kinematic viscosity 0.00893 cm^2 s^{-1}, δ_h = 238 nm, correction calculated from Eq.(S4).

4. Estimation of the adhesion hydrodynamic and inertia forces on particles.

The basic assumption of the DLVO theory[2,3] is that the net interaction energy of particle with interfaces is a sum the electrostatic double-layer and the van der Waals contributions. Therefore, approximating the electrostatic component by the linear superposition approach (LSA)[2] one can formulate this postulate as follows

$$\phi_{DLVO} = \phi_e + \phi_{vdW} = \phi_0 e^{-h/L_e} - \frac{A_{123} a_p}{6h} \tag{S5}$$

where ϕ_{DLVO} is the not energy, L_e is the double layer thickness ϕ_e is the electrostatic energy, ϕ_{vdW} is the van der Waals energy, A_{123} is the Hamaker constant for the interactions of the particle with the interface through the solvent (electrolyte), $a_p = d_p/2$ is the particle radius.

$$\phi_0 = 4\pi \; \varepsilon \left(\frac{kT}{e}\right)^2 a_p Y_p Y_i \tag{S6}$$

$$Y_p = 4 \; \mathrm{th}\left(\frac{\zeta_p e}{4kT}\right);$$

$$Y_i = 4 \; \mathrm{th}\left(\frac{\zeta_i e}{4kT}\right)$$

ε is the permittivity of the medium, k is the Boltzmann constant, T is the absolute temperature, ζ_p, ζ_i are the zeta potentials of the particle and the interface, respectively, $h = z - a_p$ is the surface to surface distance between the particle and the interface.

It should also be mentioned that the expression for the van der Waals component in Eq.(S5) remains accurate for $h \ll a_p$.

The interaction force can be directly obtained from Eq.(S5) by taking the first derive in respect to the distance h

$$F = -\frac{d\phi_{DLVO}}{dh} = \frac{\phi_0}{L_e}e^{-h/L_e} - \frac{A_{123}a_p}{6h^2} \tag{S7}$$

The hydrodynamic shear force on a particle attached to the interface (sensor) is given by the formula[2]

$$F_{Sh} = 6\pi\eta a_p^2 F_8\left(h/a_p\right)G_{Sh}(h,t) \tag{S8}$$

where F_8 is the universal hydrodynamic correction function[4] and G_{Sh} is the shear rate given by Eq.(S3).

Considering Eqs.(S3, S6) on can derive the following expression for the amplitude of the shearing force

$$F_{Sh} = 6\pi\eta a_p^2 F_8(0)\left(\frac{\omega}{\nu}\right)^{1/2} V_0 e^{-\left(\frac{\omega a_p^2}{2\nu}\right)^{1/2}} \tag{S9}$$

On the other hand, the amplitude of the inertia force exerted on an attached particle due to the sensor oscillation is given by

$$F_{ih} = m_p \frac{dv}{dt} = m_p \omega V_0\, e^{-\left(\frac{\omega a_p^2}{2\nu}\right)^{1/2}} = \frac{4}{3}\pi a_p^3 \left(\rho_p - \rho_s\right)\omega V_0\, e^{-\left(\frac{\omega a_p^2}{2\nu}\right)^{1/2}} \tag{S10}$$

Comparing Eq.(S7) and Eq.(S10) one can deduce that for a given system the ratio of the shearing to the DLVO force scales up as the particle size, whereas the ratio of the acceleration to the DLVO force scales up as the square of the particle size. One can, therefore, expect that the acceleration force will dominate over the DLVO and over the shearing forces for larger particle sizes. In order to quantitatively analyze this behavior, in Table S4 these forces are compared for particle sizes used in this work.

Table S4. The interaction energy and force for the particle/silica sensor system predicted from the DLVO theory compared with the shearing and the acceleration forces.

Particle size [nm]	ζ_p [mV]	ϕ_e [kT]	ϕ_{vdw} [kT]	F_{DLVO} [dyn]	F_{Sh} [dyn]	F_{in} [dyn]
A20 [26]	71	-33	-15	-1.0×10^{-5}	1.6×10^{-7}	2.0×10^{-11}
L40 [41]	-83*	-110	-23	-2.5×10^{-5}	2.8×10^{-7}	1.8×10^{-11}
A70 [73]	74	-97	-41	-3.0×10^{-5}	1.2×10^{-6}	4.6×10^{-10}
A140 [140]	79	-200	-80	-5.9×10^{-5}	2.8×10^{-6}	3.2×10^{-9}

Footnotes: the temperature 298 K, kinematic viscosity 0.00893 cm^2 s^{-1}, δ_h = 238 nm, zeta potential of the sensor equal to -20 mV for pH 4 and 40 mV for PAH modified sensor in the case of the L40 particles (at pH 5.7), A_{123} = 1.4×10^{-20} kT, V_0 = 6 cm s^{-1}, frequency 5×10^6 s^{-1} (first overtone), F_8 =1.70.

5. Modeling Adsorption Kinetics of Particles in the QCM cell.

As discussed in Ref.[2] particle deposition kinetics under convective-diffusion transport conditions under solid substrates (for example QCM sensor) can be theoretically described using a hybrid approach exploiting the convective-diffusion equation

$$\frac{\partial n}{\partial t} = D \, \nabla^2 n - \frac{D}{kT} \nabla \cdot (\mathbf{F} \, n) - \mathbf{V} \cdot \nabla n \tag{S11}$$

where n is the number concentration of particles, t is the time, D is the translation diffusion coefficient, $\mathbf{F}$ is the external force vector (e.g. the gravitation force) rand $\mathbf{V}$ is the unperturbed (macroscopic) fluid velocity vector.

Eq.(S11) is coupled with the surface layer transport equation where the fluid convection effects are neglected[1]

$$j_a = \frac{1}{S_g} \frac{d\Theta}{dt} = k_a \, n(\delta_a) \, B(\Theta) - \frac{k_d}{S_g} \Theta \tag{S12}$$

where j_a is the net adsorption/desorption flux, S_g is the characteristic cross-section of the particle, $\Theta = S_g N_p$ is the macromolecule coverage, N_p is the particle surface concentration, k_a, k_d are the adsorption and desorption constants, $n(\delta_a)$ is the number concentration of particles at the adsorption boundary layer of the thickness δ_a and $B(\Theta)$ is the generalized blocking function (more appropriately referred to as the available surface function).

Eq.(S12) is used as the boundary condition for the bulk mass transfer equations, Eq.(S11).

Under convective transport, where the particle concentration $n(\delta_a)$ remains in a local equilibrium with the surface coverage, the constitutive expression for the adsorption flux, Eq.(S12) becomes[2]

$$j_a = \frac{K \, B(\Theta) - K_d \Theta}{(K-1)B(\Theta)+1} k_c n_b \tag{S13}$$

where $K = k_a / k_c$ is the dimensionless coupling constants, $K_d = k_d/(S_g k_c n_b)$ is the dimensionless desorption constant, and k_c is the bulk transfer rate constant, known in analytical form for many types of flows and n_b is the bulk number concentration of particles.

Eq.(S3) can be integrated, which yields the following dependence

$$\int_{\Theta_0}^{\Theta} \frac{(K-1)B(\Theta') + 1}{K B(\Theta') - K_d \Theta'} \, d\Theta' = S_g k_c n_b t \tag{S14}$$

where Θ_0 is the initial coverage of particles.

Eq.(S14) represents a general solution for particle deposition kinetics under convection driven transport. However, it can only be evaluated by numerical integration methods if the blocking function is known in an analytical form.

It is interesting to mention that in the case of particle desorption run where the bulk concentration n_b vanishes, Eq.(S14) simplifies to the form

$$\int_{\Theta_0}^{\Theta} \frac{(k_a - k_c)B(\Theta') + k_c}{\Theta'} \, d\Theta' = -k_d k_c t \tag{S15}$$

assuming that the blocking function does not change much during the desorption run and is equal to B_0 one can integrate Eq.(S15) to the useful form

$$\Theta = \Theta_0 \, e^{-\frac{k_c}{K_a B_0 (1 - k_c/k_a)} t} \tag{S16}$$

where $K_a = k_a/k_d$ is the equilibrium adsorption constant.
Hence, the characteristic desorption time is given by

$$t_d = K_a B_0 (1 - k_c / k_a) / k_c \tag{S17}$$

It is useful to express Eq.(S14) in terms of the mass coverage of particles connected with the dimensionless coverage by

$$\Gamma = (\Theta / S_g) \, m_1 \tag{S18}$$

where m_1 is the mass of a single particle.

It should be mentioned that in terms of the QCM nomenclature, the coverage Γ is the so called 'dry' mass.

Using this definition one can express Eq.(S14) in the form

$$\int_{\Gamma_o}^{\Gamma} \frac{\left(k_a - k_c\right) B\left(\Gamma^{'}\right) + k_c}{k_a c_b B\left(\Gamma^{'}\right) - k_d \Gamma^{'}} d\Gamma = k_c t \tag{S19}$$

where $c_b = m_1 n_b$ is the mass concentration of particles in the bulk.

In a general case Eq. (S19) can be solved by numerical integration if the kinetic constants, the blocking function and the maximum coverage are known[5]. However, for bulk transport controlled regime characterized by the condition $k_a >> k_c$ and a lower coverage range, Eq. (S19) simplifies to the linear form

$$\Gamma = k_c c_b t \tag{S20}$$

The adsorption and the desorption constants appearing in Eq.(S19) are given in the general case by the expressions[2]

$$k_a^{'} = \frac{e^{\phi(\delta_a)/kT}}{\displaystyle\int_{\delta_m}^{\delta_a} \frac{e^{\phi(z')/kT}}{D(z')} dz'} \tag{S21}$$

$$k_d^{'} = k_a^{'} \, e^{\left[\phi(\delta_m) - \phi(\delta_a)\right]/kT} \tag{S22}$$

where $\phi\left(\delta_m\right)$ is the specific interaction energy of the particle with the interface evaluated at the distance δ_m (the primary minimum distance), $\phi\left(\delta_a\right)$ is the specific interaction energy of

the particle with the interface evaluated at the distance δ_a and $D(z)$ is the diffusion coefficient of the particles (a scalar quantity), which depends on the distance from the substrate surface.

Often the interaction energy around the primary minimum and the barrier region can be approximated by a parabolic distribution. Consequently the kinetic adsorption constants can be approximated by[2]

$$k_a = D(\delta_b)\left(\frac{\gamma_b}{2\pi kT}\right)^{1/2} e^{-\phi_b/kT} \cong \frac{D_\infty}{a}\left(\frac{\phi_b}{\pi kT}\right)^{1/2} e^{-\phi_b/kT}$$

$$k_d = k_a\left(\frac{\gamma_m}{2\pi kT}\right)^{1/2} e^{\phi_m/kT} \cong \frac{k_a}{\delta_m}\left(\frac{\phi_m}{\pi kT}\right)^{1/2} e^{\phi_m/kT} \tag{S23}$$

where

$$\gamma_b = -\left(\frac{d^2\phi}{dz^2}\right)_{\delta_b} \cong \frac{2\phi_b}{kT\,\delta_b^2}, \quad \gamma_m = \left(\frac{d^2\phi}{dz^2}\right)_{\delta_m} \cong \frac{2\phi_m}{kT\,\delta_m^2} \tag{S24}$$

and $D(\delta_b)$ is the value of the diffusion coefficient approximated within the barrier region according to the lubrication theory by the formula $D(\delta_b) = (\delta_b/a)D_\infty$.

It should be mentioned that for a barrier-less adsorption regime the kinetic adsorption constant can be calculated from the dependence[2]

$$k_a = \frac{D}{\delta_a(1+0.5\,\ln\delta_a/\delta_m)} \tag{S25}$$

It is interesting to calculate the characteristic desorption times for the above DLVO energy minima listed in Table S4. Considering that for the A20 particles $\phi_{DLVO} = -45$ kT, $k_c = 8.48\times10^{-5}$ cm s^{-1} and calculating k_a, k_d from Eq.(S23) one can predict Eq.(S19) that the desorption time is equal to 3×10^{15} s (for $B_0 = 0.5$), which is an infinite value from the practical point of view. Obviously, for larger particles, the desorption time becomes many orders of magnitude larger.

Moreover, in order to explicitly calculate particle deposition kinetics from Eq.(S14) one should know the blocking function, which can be conveniently acquired from the random sequential adsorption (RSA) modeling[2,6,7]. For not too large coverage range, one can approximate the blocking function by the second order series expansion

$$B(\Theta) = 1 - C_1\Theta + C_2\Theta^2 + 0(\Theta^3) \tag{S26}$$

For spheres $C_1 = 4$ and $C_2 = 6\sqrt{3}/\pi = 3.31$.

The analytical results calculated from Eq.(S16) agree with exact data derived from RSA simulations for the lower coverage range, where $B(\Theta) > 0.3$.

On the other hand, for coverages approaching the jamming coverage Θ_∞, the blocking function for spheres can be approximated by the expression

$$B(\Theta) = 2.31\left(1 - \frac{\Theta}{\Theta_\infty}\right)^3 \tag{S27}$$

In the case of spheres, one can also formulate an analytical expression fitting well the exact numerical data for the entire range of coverage[7]

$$B(\Theta) = \left[1 + 0.812\overline{\Theta} + 0.4258\left(\overline{\Theta}\right)^2 + 0.0716\left(\overline{\Theta}\right)^3\right]\left(1 - \overline{\Theta}\right)^3 \tag{S28}$$

where $\overline{\Theta} = \dfrac{\Theta}{\Theta_\infty}$.

It was shown in Ref.[1] that the above results obtained pertinent to hard particles can also be extended to the case of particles interacting via the short- range Yukawa potential. For electrostatic double-layer interactions the characteristic range of this potential is given by

$$h^* = \frac{Le}{d_p}\left[\ln\frac{\phi_o}{\phi_{ch}} - \ln\left(1 + \frac{Le}{d_p}\ln\frac{\phi_o}{\phi_{ch}}\right)\right] \tag{S29}$$

where ϕ_o is electrostatic energy at contact and ϕ_{ch} is the characteristic interaction energy.

Consequently, one can calculate the jamming coverage for interacting particles referred to as the maximum coverage) from the relationship

$$\Theta_{mx} = \Theta_\infty \frac{1}{(1+h^*)^2} \tag{S30}$$

Upon calculating Θ_{mx} one can use Eq.(S28) to calculate the blocking function substituting

$$\overline{\Theta} = \frac{\Theta}{\Theta_{mx}} .$$

6. Definitions of solvation functions

In this section main factors and functions used for expressing the amount of a solvent hydrodynamically coupled with particles deposited on the QCM sensor are defined.

The solvent mass factor, in the case of aqueous solutions referred to as the water factor is defined as

$$w = \frac{m_s + m_p}{m_p} = \frac{\Gamma_Q}{\Gamma} \tag{S31}$$

where m_s is the solvent mass associated with one particle of the mass m_p and Γ_Q is the 'wet' coverage determined by QCM.

The commonly used hydration function H, which represents the ratio of the coupled mass to the QCM wet mass is given by[8-9]

$$H = 1 - \frac{\Gamma}{\Gamma_Q} = 1 - 1/w \tag{S32}$$

Another useful function is defined as the ratio of the associated solvent volume to the particle volume[10]

$$\overline{v} = \frac{v_s}{v_p} = \frac{\rho_p}{\rho_s} \frac{m_s}{m_p} = \frac{\rho_p}{\rho_s}(w-1) = \frac{\rho_p}{\rho_s}(\frac{\Gamma_Q}{\Gamma}-1) = \frac{\rho_p}{\rho_s}\left[\frac{H}{1-H}\right] \tag{S33}$$

where v_s is the coupled solvent volume, v_p is the particle volume, ρ_p is the particle density and ρ_s is the solvent (water) density.

It should be mentioned that in contrast to H, the v function (also denoted as H_v, φ_v [8,10]) is more unique since it does not depend on the particle and solvent densities.

Except for the above functions commonly used in the literature we should define in this work a more specific function, giving the average coupled solvent level in the particle monolayer, see Figure S5.
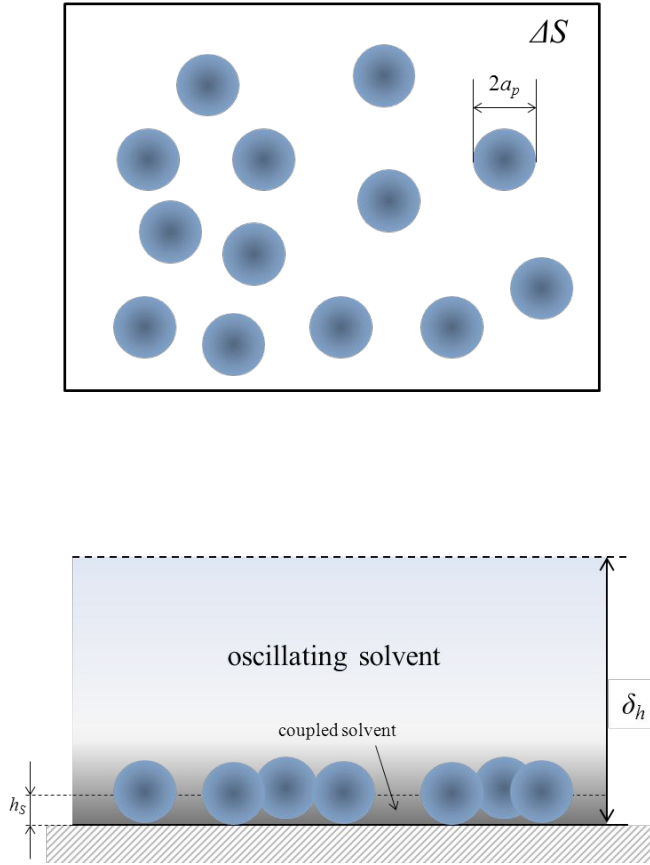
Figure S4. A schematic representation of the average coupled solvent level in the particle monolayer.

The starting point is the coupled water balance expressed as

$$N_p v_p \bar{v} = \Delta S\, h_s - N_p v_{pi}(h_s) \tag{S34}$$

where ΔS is the substrate (sensor) area, h_s is the average level of coupled water and $v_{pi}(h_s)$ is the volume of the particle immersed in the stagnant solvent.

Considering that $N_p = \dfrac{\Delta S}{S_g}\Theta$, Eq.(S34) becomes

$$\frac{\Delta S}{S_g}\Theta\, v_p \bar{v}(\Theta) = \Delta S\, h_s - \frac{\Delta S}{S_g}\Theta\, v_p(h_s) \tag{S35}$$

Additionally, defining the scaled solvent level function

$$\bar{h} = \frac{h_s}{a_p} \tag{S36}$$

where a_p is the particle radius, one can transform Eq.(S35) to the implicit dependence

$$\bar{h} - \frac{v_p}{S_g a_p} - \Theta\,\bar{v}(\Theta) - \frac{v_p}{S_g a_p}\,\Theta\,\bar{v}_{pi}(\bar{h}) = 0 \tag{S37}$$

where $\bar{v}_{pi} = v_{pi} / v_p$

For spheres one has

$$\frac{v_p}{S_g a_p} = \frac{4}{3} \tag{S38}$$

$$\bar{v}_{pi} = \frac{1}{4}\bar{h}^2 (3 - \bar{h})$$

Therefore, Eq.(S37) can be explicitly expressed in terms of $\bar{h}$, in the following form

$$\bar{h}^3 - 3\bar{h}^2 + \frac{3}{\Theta}\bar{h} - 4\bar{v}(\Theta) = 0 \tag{S39}$$

For a small coverage range where $\theta << 1$, Eq.(S36) yields the explicit expression for $\bar{h}$

$$\bar{h} = \frac{4}{3}\bar{v}(\Theta)\,\Theta \cong \frac{4}{3}\bar{v}_0\Theta \tag{S40}$$

where $\bar{v}_0$ is the limiting value of $\bar{v}$ for $\Theta = 0$.

Eq.(S40) indicates that for $\Theta << 1$ the average solvent level linearly increases with the particle coverage.

In the general case, the third order (in respect to $\bar{h}$) equation, Eq.(S39) has the following real solution

$$\bar{h} = 1 + \left[Q^{1/2} - \frac{1}{2}q\right]^{1/3} - \left[Q^{1/2} + \frac{1}{2}q\right]^{1/3} \tag{S41}$$

$$Q = \left(\frac{p}{3}\right)^3 + \left(\frac{q}{2}\right)^2$$

$$p = 9 + \frac{3}{\Theta}$$

$$q = \frac{3}{\Theta} - 2 - 4\bar{v}(\Theta)$$

References

1. Martin, S.J.; Frye, G.C.; Ricco, A. Effect of surface roughness on the response of thickness-shear mode resonators in liquids. *Anal. Chem.* **1993**, 65, 2910-2922.
2. Adamczyk, Z. Particles at interfaces, interactions, deposition, structure. Interface science and technology series. *Elsevier*, Academic Press, **2017.**
3. Adamczyk, Z.; Sadlej, K.; Wajnryb, E.; Nattich, M.; Ekiel-Jeżewska, M.L.; Bławzdziewicz, J. Streaming potential studies of colloid, polyelectrolyte and protein deposition. *Adv. Colloid Interfac.* **2010**, 153, 1-29.
4. O'Neill, M.E. A sphere in contact with a plane wall in a slow linear shear flow. *Chem. Eng. Sci.* **1968**, 23, 1293-1298.
5. Adamczyk, Z. Kinetics of diffusion-controlled adsorption of colloid particles and proteins. *J. Colloid Interface Sci.* **2000**, 229, 477-489.
6. Talbot, J.; Tarjus G.; van Tassel, P.R.; Viot, P. From car parking to protein adsorption: an overview of sequential adsorption processes. *Colloids and Surf A.* **2000**, 165, 287-324.
7. Ricci, S.M.; Talbot, J.; Tarjus, G.; Viot, P. Random sequential adsorption of anisotropic particles. II. Low coverage kinetics. *J. Chem. Phys.* **1992**, 97, 5219-28.
8. Bingen, P.; Wang, G.; Steinmetz, N.F.; Rodahl, M.; Richter, R.P. Solvation effects in the quartz crystal microbalance with dissipation monitoring response to biomolecular adsorption. a phenomenological approach. *Anal. Chem.* **2008**, 80, 8880-8890.
9. Kubiak, K.; Adamczyk, Z.; Oćwieja, M. Kinetics of silver nanoparticle deposition at PAH monolayers: Reference QCM results. *Langmuir.* **2015**, 31, 2988-2996.
10. Macakova, L.; Blomberg, E.; Claesson, P.M. Effect of adsorbed layer surface roughness on the QCM-D response: Focus on trapped water. *Langmuir.* **2007**, 23, 12436-12444.